

## PROPERTIES OF AMORPHOUS AND MICROCRYSTALLINE SUPERCONDUCTORS\*

W. L. Johnson and S. J. Poon†

## ABSTRACT

Results of x-ray diffraction, electrical resistivity, critical field ( $H_{c2}$ ) and transport measurements are presented and discussed for bulk amorphous and microcrystalline transition metal alloys obtained by liquid quenching. The transition temperature of the alloys is in the range 1.5 to 4.7°K. It is observed that  $J_c - H_{c2} - T_c$  relations are rather simple for this class of material. These relations are compared with the theories of type II superconductors wherever possible. The high resistance of bulk metallic glass to radiation damage might render them suitable for magnetic field applications in high radiation environments.

## INTRODUCTION

Superconductivity in amorphous and highly disordered thin films obtained by vapor quenching have been reported in the literature.<sup>1-5</sup> Recently, we have prepared bulk amorphous Au-La, and microcrystalline Nb-Ni, Nb-Rh and Pd-Zr superconducting alloys by the method of liquid quenching.<sup>4</sup> These alloys are stable at room temperature and have a density comparable to that of the corresponding equilibrium crystalline alloys.<sup>5</sup> We have studied the structure, electrical resistivity, upper critical magnetic field  $H_{c2}$  and transport properties of the alloys and investigated the possibility of obtaining high  $T_c$  amorphous superconductors for technical applications.

## ALLOY PREPARATION AND STRUCTURE

The detailed preparation procedures of alloys have been given in reference 6. The composition ranges for amorphous and microcrystalline phases are given in reference 4 and 6. Results of x-ray diffraction studies show broad diffuse bands. A summary of x-ray diffraction results of these phases is given in Table I. The nearest neighbor distance

TABLE I. Summary of X-ray Diffraction Results

Alloy	Nearest Neighbors Distance (Å)	Effective Microcrystal Size (Å)
Au <sub>24</sub> La <sub>76</sub>	3.55	17.5
Nb <sub>55</sub> Rh <sub>45</sub>	2.73	24
Nb <sub>55</sub> Ni <sub>15</sub> Rh <sub>30</sub>	2.66	18
Nb <sub>50</sub> Ni <sub>40</sub>	2.66	20
Pd <sub>30</sub> Zr <sub>70</sub>	3.00	27

(NND) and the effective microcrystal size ( $\mu_{eff}$ ) were calculated from the Debye formula and the Sherrer formula respectively. The effective microcrystal size ranges from 4.9 to 9 NND. Previously reported amorphous metal alloys obtained by liquid quenching can all be characterized by  $\mu_{eff}$  ranging

Manuscript received September 30, 1974.

\*Work supported by the U. S. Atomic Energy Commission.

†W. M. Keck Laboratory of Engineering Materials, California Institute of Technology, Pasadena, California 91109

from 4-5.5 NND.<sup>7</sup> When  $\mu_{eff}$  exceeds  $\sim 6$  NND, it is no longer clear that the term "amorphous" is appropriate for describing the structure of the phase. Using this rather arbitrary criteria implies that of the alloys studied, only Au-La alloys can be described as amorphous while the rest of the alloys should appropriately be described as microcrystalline.

Annealing the Au-La amorphous alloy, and the Nb-Ni, Nb-Rh and Pd-Zr microcrystalline alloys for periods of the order of 24 hours at 100°C, 600°C, 650°C and 300°C respectively results in the decomposition into more stable crystalline phases.

## ELECTRICAL PROPERTIES

The resistivity  $\rho$  (T) for amorphous Au<sub>24</sub>La<sub>76</sub> and microcrystalline Nb<sub>55</sub>Rh<sub>45</sub> together with that of crystalline samples are presented in Figures 1 (a) and 2 (a) respectively. The crystalline samples were

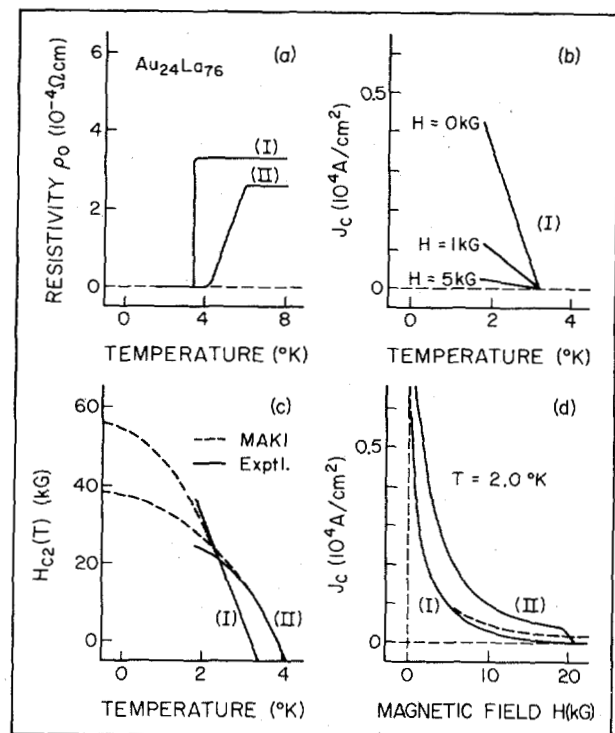


Fig. 1. Results of electrical resistivity, critical magnetic field and transport properties measurements for (I) amorphous and (II) highly crystallized Au<sub>24</sub>La<sub>76</sub> alloys.

prepared by liquid quenching the alloys at a slower cooling rate. The alloys listed in Table I can all be characterized by a well defined  $T_c$  with a transition width  $\Delta T_c$  less than 0.4°K. The  $T_c$  for Nb<sub>50</sub>Ni<sub>40</sub> and Pd<sub>30</sub>Zr<sub>70</sub> were found to be 1.5°K and 2.8°K respectively. Detailed results of electrical resistivity measurements for amorphous Au-La alloys can be found in reference 6. The residual resistivity  $\rho_0$  measured at 10°K and the temperature coefficient of

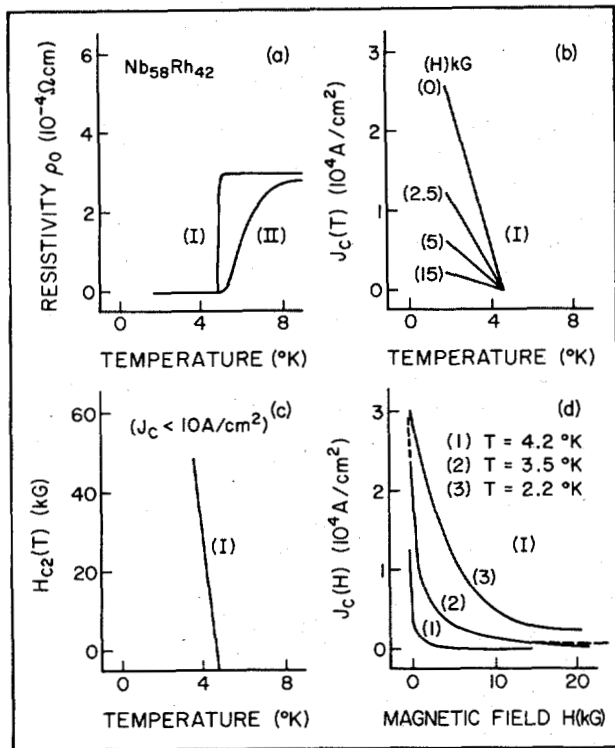


Fig. 2. Results of electrical resistivity, critical magnetic field and transport properties measurements for (I) microcrystalline  $Nb_{58}Rh_{42}$  alloy. Result of electrical resistivity measurement for (II) highly crystallized  $Nb_{58}Rh_{42}$  alloy is also included in (a).

resistivity  $1/\rho_0 \times d\rho(T)/dT$  for the alloys studied are  $\sim 10^{-4} \Omega cm$  and  $\sim 10^{-4} / ^\circ K$  respectively characteristic of a glassy metal. A change in sign in the temperature coefficient of resistivity as a function of composition was also observed for amorphous Au-La alloys. This effect has been discussed in terms of structural scattering of electrons for glassy metals in the literature.<sup>8</sup>

#### CRITICAL MAGNETIC FIELD AND TRANSPORT PROPERTIES

The magnetic properties and the characteristic intrinsic parameters  $\xi$  (coherence length),  $\lambda$  (penetration depth) and  $l$  (electronic mean free path) of amorphous Au-La alloys are discussed in reference 6, along with type II behavior of the alloys characterized by a very large Ginzburg-Landau parameter  $\kappa \sim 70$ . A similar argument based on measured residual resistivity and critical field  $H_{c2}(T)$  leads to the conclusion that comparable values of  $\kappa$  can be used to characterize the microcrystalline alloys. The  $H_{c2}(T)$  curves for amorphous  $Au_{24}La_{76}$  and microcrystalline  $Nb_{58}Rh_{42}$  are shown in Figures 1(c) and 2(c) respectively. Linear behavior was observed in the amorphous and microcrystalline samples throughout the measured ranges of temperature ( $0.5 T_c \lesssim T < T_c$ ) and magnetic fields ( $\lesssim 44 kG$ ). This behavior is apparently general for this class of materials. The dashed lines in Figure 1(c) were obtained by fitting the data to the Maki Theory<sup>9</sup> using the relation

$$\log(1/t) = \psi \left( 1 + eDH_{c2}/2\pi\kappa_B T_c t \right) - \psi \left( \frac{1}{2} \right) \quad (1)$$

where  $t = T/T_c$ ,  $D = \frac{1}{3} V_F l$  is the diffusivity and  $\psi$

is the digamma function. This expression reduces to

$$H_{c2}(t) = \frac{4k_B T_c}{\pi e} (c/D) (1-t) \left[ 1 - \left( \frac{1}{2} - \frac{28}{\pi} \zeta(3) \right) (1-t) \right] \quad (2)$$

for  $t \rightarrow 1$ .

From (2), we obtain an expression for the gradient of  $H_{c2}$  at  $t = 1$ .

$$\left( \frac{dH_{c2}(T)}{dT} \right)_{T=T_c} = - \frac{4k_B c}{\pi e D} \quad (3)$$

Expressions (2) and (3) should be valid for the present case where  $l \ll \xi_0$ . Linearity of  $H_{c2}(T)$  for the amorphous samples extends to lower temperatures than predicted by equation (1). For the disordered crystalline sample, equation (1) predicts a larger  $H_{c2}(T)$  than observed for  $H_{c2}(T)$  below  $T \approx 2.5^\circ K$ . Werthamer<sup>10</sup> has extended equation (1) to include both the paramagnetic and spin-orbit scattering effects. The spin-orbit scattering effect has been used to explain the linearity of  $H_{c2}(T)$  over a wide temperature range observed for highly disordered thin films.<sup>11</sup> It is interesting to note that the spin-orbit scattering effect is apparently more pronounced in amorphous alloys than disordered crystalline alloys.

Using the observed values of  $(-dH_{c2}(T)/dT)_{T=T_c}$  and equation (3), one can calculate the electronic diffusivity  $D$  for the alloys. Results of critical field gradient and electronic diffusivity as a function of nearest neighbor distance are shown in Figure 3. A

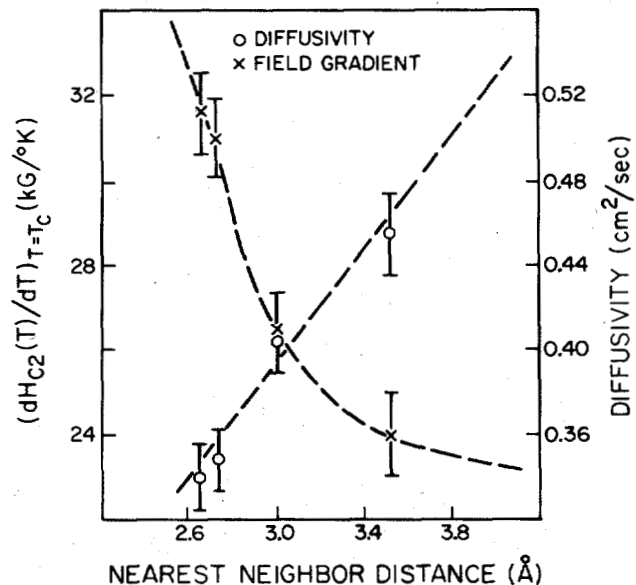


Fig. 3. Critical field gradient for amorphous  $Au_{24}La_{76}$ , microcrystalline  $Nb_{58}Ni_{16}Rh_{26}$ ,  $Nb_{58}Rh_{42}$  and  $Pd_{30}Zr_{70}$  alloys as a function of nearest neighbors distance. Electronic diffusivity for the same alloys as a function of NND is also presented.

nearly linear relation between  $D$  and NND is observed. A straight line of the form  $D \approx 0.134 \text{ NND}$  is obtained by using the least square fit. It has been suggested in reference 4 that this is related to the degree of localization of d-electron bonding states. It is worth noting that the largest gradient  $(-dH_{c2}(T)/dT)_{T=T_c}$

obtainable in the amorphous or microcrystalline alloys based on Figure 3 would be of the order of  $36 \text{ kg}/^\circ K$  taking a minimum NND to be  $\sim 2.4 \text{ \AA}$ .

Incidentally, the gradient observed in thin films of  $\text{NbN}^{11}$  ( $T_c = 15.5^\circ\text{K}$ ,  $\rho_0 \cong 2.5 \times 10^{-4} \Omega\text{cm}$ ) has a value of  $34.8\text{kG}/^\circ\text{K}$  corresponding to a NND of  $\sim 2.35\text{\AA}$ .

Critical current density measurements  $J_c(T)$  and  $J_c(H)$  for amorphous  $\text{Au}_{24}\text{La}_{76}$  and microcrystalline  $\text{Nb}_{58}\text{Rh}_{42}$  are shown in Figures 1(b), (d) and 2(b), (d) respectively. The  $J_c(H)$  curve for crystallized sample of  $\text{Au}_{24}\text{La}_{76}$  quenched at a slower cooling rate is also shown in Figure 1(d). The behavior of  $J_c(T)$  was found to be linear for both alloys over the temperature range investigated. The maximum measured  $J_c$  (at  $T \sim 2^\circ\text{K}$  and  $H = 0$ ) are about  $10^4 \text{ A/cm}^2$  for amorphous  $\text{Au}_{24}\text{La}_{76}$  and  $3 \times 10^4 \text{ A/cm}^2$  for microcrystalline  $\text{Nb}_{58}\text{Rh}_{42}$ . For the amorphous and microcrystalline samples,  $J_c(H)$  goes approximately like  $H^{-1}$  characteristic of an ideal type II superconductor. When the lattice of a superconductor is disordered on a scale much smaller than the coherence length  $\xi$  so that there are no favorable centers for flux pinning, the behavior of  $J_c(H)$  is expected to be governed by the Lorentz force of magnitude  $J_c(T)H_{c2}(T) = \alpha(T)^{1/2}$  where  $\alpha(T)$  is a temperature dependent constant. Such a relation is observed in the Figures. By comparison, the partially crystallized sample of  $\text{Au}_{24}\text{La}_{76}$  exhibits noticeable flux pinning behavior.

#### TECHNICAL APPLICATIONS

The factors which determine the usefulness of a bulk ductile superconductor are:

- (1) The value of the upper critical field gradient  $(-dH_{c2}(T)/dT)_{T=T_c}$  and the behavior of  $H_{c2}(T)$ .
  - (2) The transition temperature  $T_c$ .
  - (3) The behavior of  $J_c(H)$  at constant temperature.
- We have already estimated that the maximum upper critical field gradient obtainable is  $\sim 36\text{kG}/^\circ\text{K}$  and the linearity of  $H_{c2}(T)$  is a common property of this class of material. It has been pointed out in reference 4 that the maximum  $T_c$  is limited to  $\lesssim 10^\circ\text{K}$ . We have observed a hyperbolic relation between  $J_c$  and  $H$  which is characteristic of an ideal type II superconductor. The absence of flux pinning center leads to a rather low  $J_c$  for large  $H$ . In order to improve the  $J_c(H)$  behavior for applications, one might introduce flux pinning centers by partially crystallizing the amorphous phase. Finally, the superconducting properties of this class of material are expected to be insensitive to radiation (e.g. neutron irradiation) as shown by radiation experiments on amorphous Pd-Si alloys.<sup>13</sup>

#### CONCLUSION

Amorphous and microcrystalline bulk superconductors have been obtained by liquid quenching. It has been observed that  $T_c$ - $J_c$ - $H_{c2}$  relations for this class of material are rather simple (either hyperbolic or linear). Further investigation of this class of alloys is necessary to understand their physical properties in more detail.

#### ACKNOWLEDGEMENT

The authors wish to express their appreciation to Professor Pol Duwez for his encouragement and support throughout this work.

#### REFERENCES

1. W. Buckel and R. Hilsch, Z. Physik 138, 109 (1954).
2. W. Buckel and R. Hilsch, Z. Physik 138, 118 (1954).
3. M. M. Collver and R. H. Hammond, Phys. Rev. Letters 30, 92 (1973).
4. W. L. Johnson and S.J. Poon, to be published.
5. J. Logan, Scripta Metallurgica 8, 727 (1974).
6. W. L. Johnson, S. J. Poon and P. Duwez, to be published in Phys. Review.
7. R. C. Crewdson, Ph.D. Thesis (California Institute of Technology, 1968) (unpublished).
8. A. K. Sinha, Phys. Rev. 1, 4541 (1970).
9. K. Maki, Physics 1, 127 (1964).
10. E. Helfand and N. R. Werthamer, Phys Rev. 147, 288 (1966).
11. M. Ashkin, D. W. Deis, J. R. Gavaler and C. K. Jones, Superconductivity in d and f Band Metals, (AIP Conference Proceedings No. 4, 1972).
12. D. Saint-James, G. Sarma and E. J. Thomas, "Theory of Type II Superconductivity", Pergamon Press, Oxford (1969).
13. M. D. Lesueur, C. R. Acad. Sci., Paris 266, 1038 (1968).